# Reexamination of nuclear quadrupole moments in $^{39-41}$K isotopes

Yashpal Singh,* D. K. Nandy, and B. K. Sahoo†
*Theoretical Physics Division, Physical Research Laboratory, Navrangpura, Ahmedabad 380009, India*
(Received 20 August 2012; published 24 September 2012)

Nuclear quadrupole moments ($Q$'s) in three isotopes of the potassium atom (K) with mass numbers 39, 40, and 41 are evaluated more precisely in this work. The $Q$ value of $^{39}$K is determined to be 0.0614(6) $b$ by combining the available experimental result of the electric quadrupole hyperfine structure constant ($B$) with our calculated $B/Q$ result of its $4P_{3/2}$ state. Furthermore, combining this $Q$ value with the measured ratios $Q(^{40}\mathrm{K})/Q(^{39}\mathrm{K})$ and $Q(^{41}\mathrm{K})/Q(^{39}\mathrm{K})$, we obtain $Q(^{40}\mathrm{K}) = -0.0764(8)\ b$ and $Q(^{41}\mathrm{K}) = 0.0747(7)\ b$, respectively. These results disagree with the sub-1% accuracy standard values recently quoted by Pyykkö [Mol. Phys. **106**, 1965 (2008)]. The calculations were carried out by employing the relativistic coupled-cluster theory at the single, double, and involving important valence triple approximation. The accuracies of the calculated $B/Q$ results can be viewed on the basis of comparison between our calculated magnetic dipole hyperfine structure constants ($A$'s) with their corresponding measurements for many low-lying states. Both $A$ and $B$ results in a few more excited states are presented. Also, we find that the latest reported experimental hyperfine structure constant results for the $4P$ states in $^{39}$K are inconsistent with our calculations.

DOI: 10.1103/PhysRevA.86.032509 PACS number(s): 31.15.aj, 21.10.Ky, 31.30.Gs, 32.10.Fn

## I. INTRODUCTION

The potassium (K) atom has three naturally abundant isotopes with atomic mass numbers 39, 40, and 41. Using the modern femtosecond laser frequency combs, polarization quantum-beat and coherent-control spectroscopy techniques, high-precision measurements of hyperfine structure constants in $4P$ and $3D$ states have been carried out [1–3]. Also, a number of measurements of these quantities were carried out in the ground and other states long ago using the atomic beam magnetic resonance and level crossing techniques (e.g., see the review article by Arimondo *et al.* [4]). Theoretical studies of these quantities are of immense interest to atomic physicists to test the accuracies of the wave functions in the nuclear region [5–7]. However, theoretical evaluation of these quantities requires atomic calculations and nuclear moments [6–9]. Nuclear magnetic moments ($\mu$'s) of the above K isotopes are known very precisely, and the reported results from various studies match reasonably well with each other [10]. On the other hand, the reported nuclear quadrupole moments ($Q$'s) from various works on these isotopes differ significantly. For example, the $Q$ value of $^{39}$K is reported as 0.049(4) $b$ [4], 0.07(2) $b$ [11], 0.0601(15) $b$ [12], and within 1% error as 0.0585 $b$ [13]. The latest result, 0.0585(6) $b$, is now considered the standard $Q$ value for $^{39}$K [10,14,15]. Accurate knowledge of the $Q$ values of these isotopes is useful in many applications. This information is interesting in order to test the potential of nuclear models [16,17], to acquire information about local symmetry [18], to discover asymmetry parameters in nuclei [19,20], to study the Mossbauer spectroscopy for the structural determination of the element containing solid state compounds [21], etc.

In this paper, we analyze the electric quadrupole hyperfine structure constants for many states in K and report precise $Q$ values of its above-mentioned isotopes. As discussed later, we find the new values to be larger than the values considered standard in the literature. Atomic wave functions are calculated using the relativistic coupled-cluster (RCC) method in the Fock-space representation, and matrix elements of the hyperfine interaction Hamiltonians are estimated using these wave functions in the considered atom.

The rest of the paper is organized as follows: In the next section, we present briefly the theory of hyperfine structure in an atomic system and the single-particle matrix elements of the interaction Hamiltonians, which are used to evaluate the hyperfine structure constants. In Sec. III, we explain the RCC method briefly for the calculation of atomic wave functions. Then we present the results and a discussion before summarizing the work. Unless stated otherwise, we use atomic units (a.u.) throughout this paper.

## II. THEORY OF HYPERFINE STRUCTURE

The hyperfine structures of energy levels in an atom arise due to the interaction between electron angular momenta with nuclear spin. Details of this theory are given by Schwartz in a classic paper [22]. Mathematically, the hyperfine interaction Hamiltonian is given in a general form as noncentral interaction between electrons and the nucleus in terms of tensor operators as

$$H_{\mathrm{hfs}} = \sum_k T_e^{(k)} \cdot T_n^{(k)}, \tag{2.1}$$

where $T_e^{(k)}$ and $T_n^{(k)}$ are the spherical tensor operators of rank $k$ in the space of electronic and nuclear coordinates, respectively. In first-order perturbation theory, the hyperfine interaction energy $W_F$ of the hyperfine state $|F; IJ\rangle$ with total angular momentum $F = I + J$, with $I$ and $J$ being the nuclear spin and electronic angular momentum of the associated fine structure state $|J, M_J\rangle$, respectively, taking up to $k = 2$ is given by

$$W_F = \frac{1}{2}AR + B\frac{\frac{3}{2}R(R+1) - 2I(I+1)J(J+1)}{2I(2I-1)2J(2J-1)}, \tag{2.2}$$

*yashpal@prl.res.in
†bijaya@prl.res.in

 

with $R = F(F+1) - I(I+1) - J(J+1)$, and $A$ and $B$ are known as the magnetic dipole and electric quadrupole hyperfine structure constant for $k = 1$ and $k = 2$, respectively. The advantage of expressing the change in energy in this form is that it separates out the electronic and nuclear factors for which the calculations can be carried out with a simple approach. Here $A$ and $B$ are given by [22,23]

$$A = \mu_N g_I \frac{\langle J||T_e^{(1)}||J\rangle}{\sqrt{J(J+1)(2J+1)}} \tag{2.3}$$

and

$$B = Q\left\{\frac{8J(2J-1)}{(2J+1)(2J+2)(2J+3)}\right\}\langle J||T_e^{(2)}||J\rangle. \tag{2.4}$$

In the above expressions, $\mu_N$ and $g_I = \mu/I$ are the nuclear magneton and gyromagnetic ratio, respectively. Since our intention is to verify the accuracies of $Q$ values, we estimate $B/Q$ results in this work.

The reduced matrix elements of the electronic spherical tensor operators, $T_e^{(k)} = \sum t_e^{(k)}$, in terms of single orbitals are given by [22,23]

$$\langle\kappa_f||t_e^{(1)}||\kappa_i\rangle = -(\kappa_f+\kappa_i)\langle -\kappa_f||C^{(1)}||\kappa_i\rangle \times \int_0^\infty dr\,\frac{P_f Q_i + Q_f P_i}{r^2} \tag{2.5}$$

and

$$\langle\kappa_f||t_e^{(2)}||\kappa_i\rangle = -\langle\kappa_f||C^{(2)}||\kappa_i\rangle\int_0^\infty dr\,\frac{P_f Q_i + Q_f P_i}{r^3}, \tag{2.6}$$

where $\kappa_i$ and $P_i$ ($Q_i$) are the relativistic angular momentum quantum number and large (small) component of the Dirac spinor for the corresponding orbital $i$, respectively. The reduced matrix elements of Racah tensors ($C^{(k)}$) are given by [24]

$$\langle\kappa_f||C^{(k)}||\kappa_i\rangle = (-1)^{j_f+1/2}\sqrt{(2j_f+1)(2j_i+1)} \times \begin{Bmatrix} j_f & k & j_i \\ 1/2 & 0 & 1/2 \end{Bmatrix}\pi(\ell_f,k,\ell_i) \tag{2.7}$$

with the angular momentum selection rule $\pi(\ell_f,k,\ell_i) = 1$ when $\ell_f + k + \ell_i =$ even for the orbital angular momenta $\ell_f$ and $\ell_i$; otherwise it is zero.

## III. METHODS FOR CALCULATIONS

### A. Single-particle orbital generation

Accurate generation of atomic orbitals in the nuclear region is very important for the present study. We consider here Gaussian-type orbitals (GTO's), which provide a natural description of relativistic wave functions within the nucleus [25–27] as a basis to construct the mean-field orbitals in the Dirac (Hartree)-Fock (DF) approach. Kinetic balanced conditions between the large and small components of the Dirac spinor are imposed to ensure correct nonrelativistic behavior of the orbitals [27,28]. GTO's to construct an orbital at a particular location $r_i$ are defined as

$$F^{L(S)}(r_i) = \sum_k \mathcal{N}_k^{L(S)} r_i^{\ell+1} e^{-\eta_k r_i^2}, \tag{3.1}$$

TABLE I. $\zeta$ and $\nu$ parameters used for different $\ell$ symmetries to construct GTO's.

| | $s$ | $p$ | $d$ | $f$ | $g$ |
|---|---|---|---|---|---|
| $\zeta$ | 0.0002 | 0.0004 | 0.0003 | 0.0005 | 0.0004 |
| $\nu$ | 1.917 | 1.79 | 1.77 | 1.76 | 1.75 |

where $L(S)$ represents the large (small) component, $k$ denotes the number of GTO's, $\mathcal{N}$ corresponds to the normalization factor for each GTO, and $\eta_k$ is an arbitrary parameter which has to be chosen suitably for orbitals from different $\ell$ symmetries. To get more flexibility in optimization of our basis sets, we use the even tempering condition by defining two more parameters $\zeta$ and $\nu$ as

$$\eta_k = \zeta\,\nu^{k-1}. \tag{3.2}$$

The radial grid points $r_i$ are defined as

$$r_i = r_0[e^{h(i-1)} - 1], \tag{3.3}$$

where $r_0$ is the starting radial function taken inside the nucleus to be $2 \times 10^{-6}$ at which the wave functions become finite, and $h$ is a step size which is defined by taking the maximum radial function $r_{\max}$ as 150.0 a.u. and total grid points 1000.

We have considered 40 GTO's for each $\ell$ symmetry orbital; the considered $\zeta$ and $\nu$ are given in Table I for different $\ell$ values. Due to limitations of computational resources and negligible contributions from the high-lying virtual orbitals, we have taken up to 24 orbitals from $s$, $p$, $d$ symmetries and 17 orbitals from $f$, $g$ symmetries to construct active space for RCC calculations.

In addition, the orbitals are generated by accounting the finite size of the nucleus assuming a two-parameter Fermi nuclear charge distribution given by

$$\rho(r_i) = \frac{\rho_0}{1 + e^{(r_i - c)/a}}, \tag{3.4}$$

where $\rho_0$ is the density for the point nuclei and $c$ and $a$ are the half-charge radius and skin thickness of the nucleus, respectively. These parameters are chosen as

$$a = 2.3/4(\ln 3) \tag{3.5}$$

and

$$c = \sqrt{\frac{5}{3}r_{\rm rms}^2 - \frac{7}{3}a^2\pi^2}, \tag{3.6}$$

where $r_{\rm rms}$ is the root mean square radius of the atomic nucleus which is taken as 3.61 fm [29] for the considered atom.

### B. Calculation of atomic wave functions

To calculate the matrix elements of the hyperfine interaction Hamiltonian, we use the RCC method, where we define atomic wave functions for the considered states with valence orbital denoted by $v$ as [30,31]

$$|\Psi_v\rangle = e^T\{1 + S_v\}|\Phi_v\rangle, \tag{3.7}$$

where the DF wave function $|\Phi_v\rangle$ is constructed as $|\Phi_v\rangle = a_v^\dagger|\Phi_0\rangle$ with $|\Phi_0\rangle$ as the DF wave function for the closed-shell configuration $[3p^6]$ in the considered K atom. In the above expression, $T$ and $S_v$ are the excitation operators that

account for core and core-valence correlations to all orders, respectively. Since K is a small atom, correlation effects among electrons are expected to be less. Therefore, the role of the higher-order configurations in determining atomic wave function could be negligible. On the other hand, consideration of these configurations is computationally very expensive. Owing to this fact we account for only all possible single and double configuration excitations to all orders (known as the CCSD method) by expressing the above operators in the Fock space representation as

$$T = T_1 + T_2 = \sum_{a,p} a_p^\dagger a_a t_a^p + \frac{1}{4}\sum_{ab,pq} a_p^\dagger a_q^\dagger a_b a_a t_{ab}^{pq}, \quad (3.8)$$

$$S_v = S_{1v} + S_{2v} = \sum_{a,p} a_p^\dagger a_v s_v^p + \frac{1}{2}\sum_{ab,pq} a_p^\dagger a_q^\dagger a_b a_v s_{vb}^{pq}, \quad (3.9)$$

where the $(a,b,c,\ldots)$, $(p,q,r,\ldots)$, and $(v)$ subscripts of the second quantized operators represent core (hole), particle (virtual), and valance orbitals, respectively. However, expanding Eq. (3.7) using these CCSD operators to all nonlinear terms give rise to contributions from higher excitations. We determine the above $t$ and $s_v$ coefficients which correspond to the excitation amplitudes using the following equations:

$$\langle \Phi^L | \{\widehat{H_N e^T}\} | \Phi_0 \rangle = 0 \quad (3.10)$$

and

$$\langle \Phi_v^L | \{\widehat{H_N e^T}\} S_v | \Phi_v \rangle = -\langle \Phi_v^L | \{\widehat{H_N e^T}\} | \Phi_v \rangle + \langle \Phi_v^L | S_v | \Phi_v \rangle \Delta E_v, \quad (3.11)$$

where the superscript $L(=1,2)$ represents the single and double excited configurations from the corresponding DF states, the wide-hat symbol denotes the linked terms, $\Delta E_v$ is the attachment energy of the valence electron $v$, and $H_N$ denotes the normal ordering atomic Dirac-Coulomb Hamiltonian $H$, which is taken as

$$H = \sum_i [c\boldsymbol{\alpha}_i \cdot \boldsymbol{p}_i + (\beta_i - 1)c^2] + \sum_{i \geqslant j} \frac{1}{r_{ij}}, \quad (3.12)$$

where $\boldsymbol{\alpha}$ and $\beta$ are the usual Dirac matrices and $c$ is the velocity of light. $\Delta E_v$ is evaluated by

$$\Delta E_v = \langle \Phi_v | \{\widehat{H_N e^T}\} \{1 + S_v\} | \Phi_v \rangle. \quad (3.13)$$

To improve the quality of energy and calculation of wave functions due to the dominant triple excitations containing the valence orbital, we define a perturbation operator $S_{3v}$ by contracting $H_N$ with $T_2$ and $S_{2v}$ operators as

$$S_{3v}(s_{vbc}^{pqr}) = \frac{\widehat{H_N T_2} + \widehat{H_N S_{2v}}}{\epsilon_p + \epsilon_q + \epsilon_r - \epsilon_b - \epsilon_c - \epsilon_v}, \quad (3.14)$$

where $s_{vbc}^{pqr}$ corresponds to excitation amplitudes and $\epsilon_i$ is the DF energy of the electron in the $i$th orbital. This operator is considered a part of the $S_v$ operator in Eq. (3.13) to get an additional contribution to $\Delta E_v$. Since $\Delta E_v$ is involved in Eq. (3.11), we solve both of the equations simultaneously in an iterative procedure. This approach is generally referred to as the CCSD(T) method [32]. The diagrammatic representation of these excitations is shown in Fig. 1.

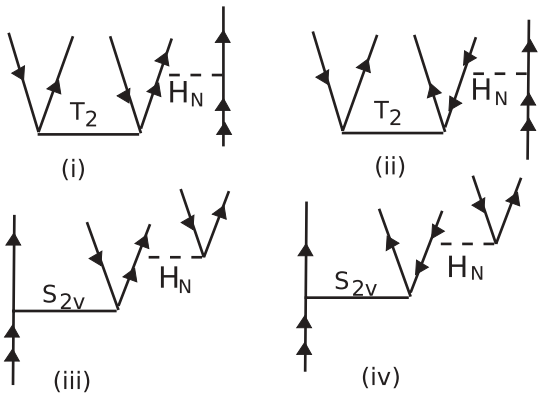


FIG. 1. Typical Goldstone diagrams representing leading-order triple excitations over the CCSD method. Double arrows in the diagrams represent valence electron $v$, and the lines with upward (downward) arrows represent particle (hole) orbitals.

The expectation values due to the hyperfine interaction operators have been evaluated using our RCC method by

$$\begin{aligned}\langle T_e^{(k)} \rangle &= \frac{\langle \Psi_v | T_e^{(k)} | \Psi_v \rangle}{\langle \Psi_v | \Psi_v \rangle} \\ &= \frac{\langle \Phi_v | \{1 + S_v^\dagger\} \overline{T}_e^{(k)} \{1 + S_v\} | \Phi_v \rangle}{\{1 + S_v^\dagger\} \overline{N}_0 \{1 + S_v\}} \\ &= \frac{\langle \Phi_v | \{1 + S_{1v}^\dagger + S_{2v}^\dagger\} \overline{T}_e^{(k)} \{1 + S_{1v} + S_{2v}\} | \Phi_v \rangle}{\{1 + S_{1v}^\dagger + S_{2v}^\dagger\} \overline{N}_0 \{1 + S_{1v} + S_{2v}\}},\end{aligned} \quad (3.15)$$

where $\overline{T}_e^{(k)} = (e^{T^\dagger} T_e^{(k)} e^T)$ and $\overline{N}_0 = e^{T^\dagger} e^T$. Generally, both $\overline{T}_e^{(k)}$ and $\overline{N}_0$ in our RCC approach are nonterminating series. These terms are terminated keeping terms minimum up to fourth order in perturbation. Description of this procedure has been given in previous works [33–35]. Contributions from the normalization of the wave functions ($x_{\rm norm}$) are estimated explicitly in the following way

$$x_{\rm norm} = \langle \Psi_v | T_e^{(k)} | \Psi_v \rangle \left\{ \frac{1}{1 + N_v} - 1 \right\}, \quad (3.16)$$

where $N_v = \{1 + S_{1v}^\dagger + S_{2v}^\dagger\} \overline{N}_0 \{1 + S_{1v} + S_{2v}\}$.

## IV. RESULTS AND DISCUSSIONS

Our aim is to obtain $B/Q$ values more accurately in different states of the K atom so that they can be combined with the available precise experimental results for $B$ to estimate $Q$. In order to verify the accuracies of the $B/Q$ results from our calculations, it would be felicitous to test the accuracies of the wave functions in the nuclear region. Owing to the fact that our calculation procedure deals with many numerical computations at different stages, along with the fact that it correlates with higher excitations configurations indirectly, it would be very difficult to estimate uncertainties from the used numerical methods and approximations taken at the level of excitations. With the intention of verifying accuracies of the wave functions in the nuclear region, we have calculated $A$ for many states in K. Assuming that the anomalous effects due to

TABLE II. Comparison of calculated and available experimental $A$ results in $^{39-41}$K (in MHz). Theoretical $A$'s in different isotopes are evaluated using the calculated CCSD(T) results of $A/g_I$ in $^{39}$K and their respective experimental $g_I$ values. Uncertainties estimated from the calculations are given in parentheses with our results. Experimental results which are not in agreement with our calculated results are given in bold fonts.

| | This work | | | Experiment | | |
|---|---|---|---|---|---|---|
| State | $^{39}$K | $^{40}$K | $^{41}$K | $^{39}$K | $^{40}$K | $^{41}$K |
| $4S_{1/2}$ | 229.6(2.0) | −285.5(2.5) | 126.0(1.1) | 230.859 860 1(3) [4] | −285.7308(24) [4] | 127.006 935 2(6) [4] |
| $4P_{1/2}$ | 27.4(5) | −34.04(62) | 15.02(27) | 27.775(42) [2] | −34.523(25) [2] | 15.245(42) [2] |
| | | | | **28.85(30)** [4] | −34.49(11) [36] | 15.19(21) [36] |
| | | | | 27.80(15) [36] | | 15.1(8) [37] |
| | | | | **28.848(5)** [3] | | |
| | | | | 27.5(4) [37] | | |
| | | | | **28.859(15)** [38] | | |
| $4P_{3/2}$ | 5.9(2) | −7.35(37) | 3.25(16) | 6.093(25) [2] | −7.585(10) [2] | 3.363(25) [2] |
| | | | | 6.06(8) [4] | −7.48(6) [36] | 3.40(8) [39] |
| | | | | 6.00(10) [40] | −7.59(6) [41] | 3.325(15) [42] |
| | | | | 6.077(23) [3] | | |
| | | | | 6.13 [39] | | |
| $3D_{3/2}$ | 1.0(2) | −1.25(25) | 0.55(11) | 0.96(4) [1] | 1.07(2) [1] | 0.55(3) [1] |
| $3D_{5/2}$ | −0.57(5) | 0.711(62) | −0.314(27) | 0.62(4) [1] | 0.71(4) [1] | 0.40(2) [1] |
| $4D_{3/2}$ | 0.686(4) | −0.853(5) | 0.377(2) | | | |
| $4D_{5/2}$ | −0.332(2) | 0.413(2) | −0.182(1) | | | |
| $5S_{1/2}$ | 55.0(1.0) | −68.4(1.2) | 30.18(55) | 55.50(60) [4] | | |
| $5P_{1/2}$ | 8.8(5) | −10.98(62) | 4.84(27) | 9.02(17) [4] | | |
| $5P_{3/2}$ | 1.9(2) | −2.37(25) | 1.04(11) | 1.969(13) [4] | −2.45(2) [4] | 1.08(2) [4] |
| | | | | 1.95(5) [40] | | |
| $5D_{3/2}$ | 0.39(5) | −0.489(62) | 0.22(27) | 0.44(10) [4] | | |
| $5D_{5/2}$ | −0.171(7) | 0.213(9) | −0.094(4) | ±0.24(7) [4] | | |
| $6S_{1/2}$ | 21.1(6) | −26.24(75) | 11.58(33) | 21.81(18) [4] | | 12.03(40) [4] |
| $6P_{1/2}$ | 3.9(4) | −4.87(50) | 2.15(22) | 4.05(7) [4] | | |
| $6P_{3/2}$ | 0.9(2) | −1.17(25) | 0.51(11) | 0.886(8) [4] | | |
| $6D_{3/2}$ | 0.24(5) | −0.297(62) | 0.131(27) | 0.25(3) [43] | | |
| | | | | ±0.2(2) [4] | | |
| $6D_{5/2}$ | −0.112(5) | 0.139(6) | −0.061(3) | −0.12(4) [43] | | |
| | | | | ±0.10(10) [4] | | |
| $7S_{1/2}$ | 10.3(5) | −12.83(62) | 5.66(27) | 10.79(5) [4] | | |
| $7P_{1/2}$ | 2.1(3) | −2.61(37) | 1.15(16) | ±2.18(5) [4] | | |
| $7P_{3/2}$ | 0.50(3) | −0.62(37) | 0.28(16) | | | |
| $7D_{3/2}$ | 0.15(1) | −0.19(12) | 0.083(5) | | | |
| $7D_{5/2}$ | −0.068(5) | 0.085(6) | −0.037(3) | | | |
| $8S_{1/2}$ | 5.8(2) | −7.27(25) | 3.21(11) | 5.99(8) [4] | | |
| $8P_{1/2}$ | 1.3(1) | −1.56(12) | 0.69(55) | | | |
| $8P_{3/2}$ | 0.301(5) | −0.374(6) | 0.165(3) | | | |
| $8D_{3/2}$ | 0.101(2) | −0.126(2) | 0.055(11) | | | |
| $8D_{5/2}$ | −0.040(1) | 0.050(1) | −0.022(1) | | | |
| $9S_{1/2}$ | 3.4(3) | −4.25(37) | 1.88(16) | | | |
| $9P_{1/2}$ | 1.0(1) | −1.19(12) | 0.53(55) | | | |
| $9P_{3/2}$ | 0.230(4) | −0.286(5) | 0.126(2) | | | |
| $9D_{3/2}$ | 0.334(4) | −0.415(5) | 0.183(2) | | | |
| $9D_{5/2}$ | −0.148(2) | 0.184(2) | −0.081(1) | | | |
| $10S_{1/2}$ | 2.2(3) | −2.68(37) | 1.18(16) | 2.41(5) [4] | | |

different nuclear sizes in all the considered isotopes are very small, we evaluate $A/g_I$ in $^{39}$K and determine $A$ values for the corresponding isotopes using their respective $g_I$ values. We have used experimental values of $g_I(^{39}K) = 0.260\,977\,2$, $g_I(^{40}K) = -0.324\,525$, and $g_I(^{41}K) = 0.143\,246\,7$ [10] to estimate these quantities, ignoring their uncertainties as they will not muddle the results within the reported uncertainties. Both the calculated and experimental results are compared in Table II. We estimate uncertainties in our calculations by considering incompleteness of basis functions, contributions from the inactive orbitals in the RCC method, and higher-order excitation levels and from the neglected terms in the nontruncative series of Eq. (3.15). The upper limits to these uncertainties are given in parentheses of Table II. There

TABLE III. Comparison between different theoretical results of $A$ in $^{39}$K (in MHz).

| | Others [44] | | | This work | | |
|---|---|---|---|---|---|---|
| State | DF | SD | SDpT | DF | CCSD | CCSD(T) |
| $4S_{1/2}$ | 146.91 | 237.40 | 228.57 | 146.794 | 229.573 | 229.556 |
| $4P_{1/2}$ | 16.616 | 28.689 | 27.662 | 16.616 | 27.247 | 27.371 |
| $4P_{3/2}$ | 3.233 | 6.213 | 5.989 | 3.234 | 5.886 | 5.913 |
| $3D_{3/2}$ | 0.447 | 0.983 | 1.111 | 0.447 | 1.006 | 1.003 |
| $3D_{5/2}$ | 0.192 | −0.535 | −0.639 | 0.192 | −0.574 | −0.572 |
| $4D_{3/2}$ | 0.281 | 0.678 | | 0.281 | 0.690 | 0.686 |
| $4D_{5/2}$ | 0.120 | −0.307 | | 0.120 | −0.334 | −0.332 |
| $5S_{1/2}$ | 38.877 | 56.102 | 54.817 | 38.847 | 55.070 | 54.981 |
| $5P_{1/2}$ | 5.735 | 9.202 | 8.949 | 5.735 | 8.755 | 8.827 |
| $5P_{3/2}$ | 1.117 | 1.988 | 1.932 | 1.117 | 1.887 | 1.903 |
| $5D_{3/2}$ | 0.168 | 0.409 | | 0.168 | 0.396 | 0.393 |
| $5D_{5/2}$ | 0.072 | −0.167 | | 0.072 | −0.173 | −0.171 |
| $6S_{1/2}$ | 15.759 | 22.025 | 21.609 | 15.105 | 21.167 | 21.10 |
| $6P_{1/2}$ | 2.629 | 4.066 | 4.014 | 2.629 | 3.874 | 3.918 |
| $6P_{3/2}$ | 0.512 | 0.874 | 0.866 | 0.512 | 0.928 | 0.937 |
| $6D_{3/2}$ | 0.105 | 0.253 | | 0.104 | 0.241 | 0.239 |
| $6D_{5/2}$ | 0.0448 | −0.0975 | | 0.045 | −0.113 | −0.112 |
| $7S_{1/2}$ | 7.900 | 10.876 | 10.690 | 7.894 | 10.363 | 10.317 |
| $7P_{1/2}$ | 1.417 | 2.191 | 2.140 | 1.417 | 2.066 | 2.095 |
| $7P_{3/2}$ | 0.276 | 0.473 | 0.462 | 0.276 | 0.495 | 0.502 |
| $7D_{3/2}$ | 0.0685 | 0.1644 | | 0.067 | 0.154 | 0.152 |
| $7D_{5/2}$ | 0.0293 | −0.0611 | | 0.028 | −0.069 | −0.068 |
| $8S_{1/2}$ | 4.511 | 6.156 | 6.057 | 4.536 | 5.880 | 5.847 |
| $8P_{1/2}$ | | | | 0.855 | 1.236 | 1.257 |
| $8P_{3/2}$ | | | | 0.166 | 0.296 | 0.301 |
| $8D_{3/2}$ | | | | 0.048 | 0.102 | 0.101 |
| $8D_{5/2}$ | | | | 0.019 | −0.040 | −0.040 |
| $9S_{1/2}$ | 2.814 | 3.818 | 3.759 | 2.685 | 3.444 | 3.420 |
| $9P_{1/2}$ | | | | 0.695 | 0.945 | 0.958 |
| $9P_{3/2}$ | | | | 0.136 | 0.227 | 0.230 |
| $9D_{3/2}$ | | | | 0.189 | 0.338 | 0.334 |
| $9D_{5/2}$ | | | | 0.083 | −0.151 | −0.148 |
| $10S_{1/2}$ | 1.871 | 2.529 | 2.491 | 1.878 | 2.171 | 2.154 |

are also a number of experimental results of these quantities reported in low-lying states. Some of these results are not in agreement within their reported uncertainties. Our estimated results for the $4P_{1/2}$ state are also not in agreement with the reported results in Refs. [3,4,38], among which the results reported in Ref. [3] are the latest.

We also compare our $A$ results for $^{39}$K obtained using the DF, CCSD, and CCSD(T) methods with other recent calculations [44] in Table III. In Ref. [44], Safronova and Safronova also used the linearized RCC method with single and double approximation (the SD method), including important triple effects for some of the states (the SDpT method). They find large differences between their SD and SDpT results in contrast to our finding of small differences between our CCSD and CCSD(T) results. However, both of the calculations reveal that the signs of the $A$ values of the $3D_{5/2}$, $5D_{5/2}$, $6D_{5/2}$, and $7P_{1/2}$ states are negative, which were not resolved correctly in the measurements. Moreover, both of the theoretical results for the $4P_{1/2}$ state are in good agreement. All of these calculations indicate that correlation effects in the considered atom are substantial, for which an all-order perturbative method like ours is suitable to determine wave functions accurately. To our knowledge, $A$ values are not known experimentally for some of the states in $^{39}$K that are reported in this work; close agreement between the results from both of the calculations for these states will be very useful in conducting new measurements in the right direction. Also, we have given $A$ values for a few excited states where neither measurements nor theoretical calculations are available.

Following $A$ results, we now present our calculated $B/Q$ results using the DF, CCSD, and CCSD(T) methods in Table IV for the states where precise experimental $B$ results for $^{39}$K and $^{41}$K are available. We also estimate the uncertainties associated with the results obtained using the CCSD(T) method and present them in parentheses in the same table. The uncertainties are estimated using the procedure we followed for $A$. To justify that trends of correlation effects for both the properties behave in a similar manner, we present contributions from various RCC terms to both $A$ and $B/Q$ results in Table V for a few important states. It is found that in states where the angular

TABLE IV. Calculated $B/Q$ values (in MHz/$b$) from our DF, CCSD, and CCSD(T) methods and accurately known experimental $B$ results (in MHz) in $^{39}$K and $^{41}$K. The most precise $B$ results and $Q$ values estimated by combining with the calculated $B/Q$ values in both the isotopes are given in bold fonts. The underlined results are more precise, but they are inconsistent with other studies.

| | | Theory | | Experiment | | Experiment | |
|---|---|---|---|---|---|---|---|
| State | DF | CCSD | CCSD(T) | $B(^{39}\mathrm{K})$ | $Q(^{39}\mathrm{K})$ | $B(^{41}\mathrm{K})$ | $Q(^{41}\mathrm{K})$ |
| $4P_{3/2}$ | 23.000 | 44.392 | 44.6(5) | **2.786(71)** [2] | **0.0625(17)** | 3.351(71) [2] | |
| | | | | 2.72(12) [38] | | 3.34(24) [39] | |
| | | | | 2.83(13) [45] | | **3.320(23)** [42] | **0.0744(10)** |
| | | | | 2.875(55) [3] | 0.0645(14) | | |
| | | | | 2.9(2) [40] | | | |
| $5P_{3/2}$ | 7.866 | 13.833 | 13.9(4) | **0.870(22)** [4] | 0.0626(22) | **1.06(4)** [39] | 0.0763(36) |
| | | | | 0.92(10) [40] | | | |
| $6P_{3/2}$ | 3.340 | 6.285 | 6.4(5) | **0.370(15)** [4] | 0.0578(51) | | |

momentum is larger than half, the contributions from the correlation effects are always of a similar scale in magnitude and the contributions coming from $\overline{O}S_{2v} + \text{c.c.}$ are larger than $\overline{O}S_{1v} + \text{c.c.}$ This implies that the core-polarization effects are large enough to estimate $B/Q$ results in the considered atom which are accounted for, up to all orders through $\overline{O}S_{2v} + \text{c.c.}$ RCC terms in our calculations. There are no other calculated results for $B/Q$ available, to our knowledge, in any of the considered isotopes of K to compare with our results.

There are also several experimental results available for $B$ in $^{39}$K as well as $^{41}$K which are given in Table IV [2–4,38–40,42,45]. The most precise values are quoted in bold fonts for the respective states except the one reported latest in Ref. [3], which is underlined in the same table (we come back to this result later). By combining these results with our calculated $B/Q$ values, we estimate $Q$'s values in the above two isotopes. We obtain three different values of $Q$ in $^{39}$K and two values in $^{41}$K. All of these estimated values agree with each other in their respective uncertainties, but the most precise results which are obtained from the $4P_{3/2}$ state are 0.0625(17) $b$ and 0.0744(10) $b$ for $^{39}$K and $^{41}$K, respectively. These results are also given in bold fonts in the above table. Here we have used the following expression to evaluate the net uncertainties of the $Q$ values:

$$\delta C = C\sqrt{\left(\frac{\delta A}{A}\right)^2 + \left(\frac{\delta B}{B}\right)^2}, \tag{4.1}$$

where we assume $C$ is the extracted value from $A/B$ and $\delta A$, $\delta B$, and $\delta C$ are their respective uncertainties.

Among both of the new $Q$ values in $^{39}$K and $^{41}$K, the relative uncertainty in $Q$ of $^{41}$K is small. Moreover, there are also experimental results for the ratios of $Q$ values between $^{39}$K, $^{40}$K, and $^{41}$K available as [46,48,49]

$$\frac{Q(^{40}K)}{Q(^{39}K)} = -1.244 \pm 0.002 \tag{4.2}$$

and

$$\frac{Q(^{41}K)}{Q(^{39}K)} = 1.2173 \pm 0.0001. \tag{4.3}$$

TABLE V. Contributions from different RCC terms to $A$ (in MHz) and $B/Q$ (in MHz/$b$), where c.c. stands for complex conjugation.

| | $\overline{O}$ | | $\overline{O}S_{1v} + \text{c.c.}$ | | $\overline{O}S_{2v} + \text{ c.c.}$ | | Others | | $x_{\text{norm}}$ | |
|---|---|---|---|---|---|---|---|---|---|---|
| State | $A$ | $B/Q$ | $A$ | $B/Q$ | $A$ | $B/Q$ | $A$ | $B/Q$ | $A$ | $B/Q$ |
| $4S_{1/2}$ | 146.576 | | 46.148 | | 33.0457 | | 6.707 | | −2.920 | |
| $4P_{1/2}$ | 16.341 | | 5.500 | | 4.820 | | 0.900 | | −0.190 | |
| $4P_{3/2}$ | 3.186 | 22.662 | 1.062 | 7.562 | 1.430 | 13.386 | 0.275 | 1.280 | −0.040 | −0.305 |
| $3D_{3/2}$ | 0.464 | 1.168 | 0.430 | 1.080 | −0.059 | 2.947 | 0.185 | 0.089 | −0.017 | −0.090 |
| $3D_{5/2}$ | 0.199 | 1.666 | 0.183 | 1.527 | −0.766 | 4.223 | −0.178 | 0.127 | 0.010 | −0.128 |
| $5S_{1/2}$ | 38.770 | | 7.898 | | 8.200 | | 0.725 | | −0.612 | |
| $5P_{1/2}$ | 5.683 | | 1.535 | | 1.571 | | 0.100 | | −0.062 | |
| $5P_{3/2}$ | 1.089 | 7.752 | 0.296 | 2.114 | 0.463 | 3.967 | 0.068 | 0.206 | −0.013 | −0.096 |
| $6S_{1/2}$ | 15.043 | | 2.882 | | 3.150 | | 0.246 | | −0.217 | |
| $6P_{1/2}$ | 2.615 | | 0.633 | | 0.630 | | 0.067 | | −0.027 | |
| $6P_{3/2}$ | 0.510 | 3.631 | 0.122 | 0.872 | 0.276 | 1.825 | 0.037 | 0.070 | −0.006 | −0.043 |
| $7S_{1/2}$ | 7.902 | | 1.148 | | 1.309 | | 0.062 | | −0.104 | |
| $8S_{1/2}$ | 4.540 | | 0.592 | | 0.746 | | 0.026 | | −0.057 | |
| $9S_{1/2}$ | 2.687 | | 0.316 | | 0.438 | | 0.011 | | −0.032 | |
| $10S_{1/2}$ | 1.880 | | 0.013 | | 0.291 | | −0.014 | | −0.015 | |

TABLE VI. Reported values of nuclear quadrupole moments $Q$ in $b$ for $^{39}$K, $^{40}$K, and $^{41}$K from various studies.

| Isotope | This work | Others |
|---|---|---|
| $^{39}$K | 0.0614(6) | 0.0585[a] [13] |
| | | 0.0601(15) [12] |
| | | 0.049(4) [46] |
| $^{40}$K | −0.0764(8) | −0.073[a] [13] |
| | | −0.0749(19) [12] |
| $^{41}$K | 0.0747(7) | 0.0711[a] [13] |
| | | 0.0733(18) [12] |

[a]Accuracy is expected to be better than 1%.

Using the measured $\frac{Q(^{41}K)}{Q(^{39}K)}$ and $Q$ value of $^{41}$K, we get a new $Q$ value for $^{39}$K as 0.0612(8) $b$. Considering both of the values of $Q$ in $^{39}$K, we restrict the lower and upper limits of $Q(^{39}\text{K})$ to 0.0608 $b$ and 0.0620 $b$, respectively. Therefore, we recommend the $Q$ value of $^{39}$K as 0.0614(6) $b$. Now with this most precise $Q$ value and the above ratios of $Q$ values between different isotopes, we get precise $Q$ values for $^{40}$K and $^{41}$K as −0.0764(8) $b$ and 0.0747(7) $b$, respectively. There are also other reported $Q$ values, which we have compared with ours in Table VI. As seen from the table, there are three other works that report these results [12,13,46]. Apart from Ref. [46], the calculations carried out in these works are rigorous, and results reported in Ref. [13] are the latest. The $Q$ values reported in Ref. [12] match our estimated values with some overlaps within the predicted uncertainties; however, results reported in Ref. [13] disagree with ours. In both of these theoretical works, they have determined electric field gradients at the nucleus to extract the nuclear quadrupole moments, and the results are model independent. But both of the calculations are less rigorous than the present calculations. In Ref. [12], Sundholm and Olsen have used a nonrelativistic large-scale finite-element multiconfiguration Hartree-Fock configuration interaction (MCHF) method. The core contributions were estimated from the core-valence correlation calculations, and the relativistic corrections are accounted for separately from the DF calculation. In contrast to this work, we have considered the core correlation and core-valence correlations to all orders, and relativistic effects are included to all orders through the RCC method. In fact, their truncative CI method is known to have size-consistent problem [50] against our RCC method. On the other hand, the level of approximations employed to carry out calculations in Ref. [13] by Kellö and Sadlej are comparable to the present work. In their work, calculations are performed with a scalar relativistic Hamiltonian using the Douglas-Kroll approach, and the CCSD(T) method is used to account for the correlation effects. Since this approach is better than the above-mentioned MHCF method, the results reported in Ref. [13] were considered to be more accurate and estimated to be within 1% accuracy. However, we find the reported values in Ref. [13] to be smaller in magnitude as compared to our estimations.

Now coming back to the results reported in Ref. [3], it was already found earlier that the reported $A$ result of the $4P_{1/2}$

TABLE VII. Comparison of estimated and experimental $B$ results in $^{39-41}$K (in MHz).

| | | This work | | | Experiments | | |
|---|---|---|---|---|---|---|---|
| State | $(B/Q)^{(\text{theor})}$ | $^{39}$K | $^{40}$K | $^{41}$K | $^{39}$K | $^{40}$K | $^{41}$K |
| $4P_{3/2}$ | 44.6(5) | 2.738(41) | −3.41(5) | 3.332(49) | 2.786(71) [2] | −3.445(90) [2] | 3.351(71) [2] |
| | | | | | 2.9(2) [40] | −3.23(50) [36] | 3.34(24) [39] |
| | | | | | 2.72(12) [39] | −3.5(5) [41] | 3.320(23) [42] |
| | | | | | 2.83(13) [4] | | |
| $3D_{3/2}$ | 5.2(5) | 0.319(31) | −0.40(4) | 0.388(38) | 0.37(8) [1] | 0.4(1) [1] | 0.51(8) [1] |
| $3D_{5/2}$ | 7.4(4) | **0.454(25)** | −0.565(31) | **0.553(30)** | <0.3 [1] | 0.8(8) [1] | <0.2 [1] |
| $4D_{3/2}$ | 2.35(4) | 0.144(3) | −0.180(4) | 0.176(3) | | | |
| $4D_{5/2}$ | 3.35(4) | 0.206(3) | −0.256(4) | 0.250(4) | | | |
| $5P_{3/2}$ | 13.9(4) | 0.853(26) | −1.06(3) | 1.038(31) | 0.870(22) [39,40] | −1.16(22) [41] | 1.06(4) [39] |
| | | | | | 0.92(10) [40] | | |
| $5D_{3/2}$ | 1.16(8) | 0.071(5) | −0.088(6) | 0.087(6) | | | |
| $5D_{5/2}$ | 1.65(10) | 0.101(6) | −0.126(8) | 0.123(8) | | | |
| $6P_{3/2}$ | 6.4(5) | 0.393(31) | −0.489(39) | 0.478(38) | 0.370(15) [47] | | |
| $6D_{3/2}$ | 0.72(5) | 0.044(3) | −0.055(4) | 0.054(4) | 0.05(2) [43] | | |
| $6D_{5/2}$ | 1.02(6) | 0.063(4) | −0.078(5) | 0.076(5) | | | |
| $7P_{3/2}$ | 3.4(3) | 0.209(19) | −0.260(23) | 0.254(23) | | | |
| $7D_{3/2}$ | 0.44(3) | 0.027(2) | −0.034(2) | 0.033(2) | | | |
| $7D_{5/2}$ | 0.62(4) | 0.038(2) | −0.047(3) | 0.046(3) | | | |
| $8P_{3/2}$ | 2.0(2) | 0.123(12) | −0.153(15) | 0.149(15) | | | |
| $8D_{3/2}$ | 0.29(2) | 0.018(1) | −0.022(2) | 0.022(2) | | | |
| $8D_{5/2}$ | 0.36(2) | 0.022(1) | −0.028(2) | 0.027(2) | | | |
| $9P_{3/2}$ | 1.5(2) | 0.092(12) | −0.115(15) | 0.112(15) | | | |
| $9D_{3/2}$ | 0.92(6) | 0.056(4) | −0.070(5) | 0.069(5) | | | |
| $9D_{5/2}$ | 1.35(8) | 0.083(5) | −0.103(6) | 0.101(6) | | | |

in that work does not agree with the present study. Again, if we use the extracted value 0.0645(14) $b$ for $Q$ of $^{39}$K and substitute it in Eqs. (4.2) and (4.3) to determine $Q$ of $^{40}$K and $^{41}$K, the results seem to be completely in disagreement with all other studies. Indeed, when these values are substituted to obtain further $B$ values, we are not able to compare the results with any experimental results. Therefore, more experimental measurements of $B$'s are necessary to resolve this inconsistency.

In view of the above inconsistency, it will also be interesting to see further theoretical studies of $B/Q$ results to draw comparison with the present work. Moreover, we combine our calculated $B/Q$ results with the newly obtained $Q$ values to determine theoretical results for $B$ in many states of the considered isotopes of K. These results are given in Table VII. We have also neglected here the anomalous effects in calculated $B/Q$ values for different isotopes due to their negligible roles. If better precise measurements of $B$ are available, then combining those results with our calculated $B/Q$ values will definitely give rise to more accurate $Q$ values in these isotopes. Also, accurate theoretical calculations of $B/Q$ results in these isotopes can also give rise to more precise $Q$ values in K. In fact, as can be noticed in Table VII, our estimated $B$ results for different states in K isotopes agree very well in most of the states except for the $3D$ states. Due to all of the above findings, we suggest further measurements of $B$ in these states to ascertain our results. Theoretical results for $B$ are also given in many excited states, which can be verified by future measurements.

## V. CONCLUSION

We have employed the relativistic coupled-cluster method to calculate matrix elements of the hyperfine interaction Hamiltonians in the potassium atom. By performing calculations of the magnetic dipole hyperfine structure constants in this atom, we have tested the accuracies of the wave functions in the nuclear region. These wave functions were further used for the electric quadrupole hyperfine interaction studies. By combining our calculations with the corresponding measurements, we obtained the nuclear quadrupole moments as 0.0614(6) $b$, −0.0764(8) $b$, and 0.0747(7) $b$ for $^{39}$K, $^{40}$K, and $^{41}$K, respectively. These results agree with one of the previous works but do not agree with others, including the latest reported results. After obtaining nuclear quadrupole moments, we substituted them to obtain electric quadrupole hyperfine structure constants in many states and found very good agreement with many of the experimental results except for the $3D$ states. Also, we find that some of the reported experimental results are in disagreement with each other and with the present work. Results in a few highly excited states are given which were not reported earlier. We suggest further studies of the considered properties to ascertain our findings.

## ACKNOWLEDGMENT

Computations were carried out using the 3TFLOP HPC cluster of Physical Research Laboratory, Ahmedabad.

[1] A. Sieradzan, R. Stoleru, W. Yei, and M. D. Havey, Phys. Rev. A **55**, 3475 (1997).
[2] S. Falke, E. Tiemann, C. Lisdat, H. Schnatz, and G. Grosche, Phys. Rev. A **74**, 032503 (2006).
[3] D. Das and V. Natarajan, J. Phys. B **40**, 035001 (2008).
[4] E. Arimondo, M. Inguscio, and P. Violino, Rev. Mod. Phys. **49**, 31 (1977).
[5] H. S. Nataraj, B. K. Sahoo, B. P. Das, and D. Mukherjee, Phys. Rev. Lett. **106**, 200403 (2011).
[6] B. K. Sahoo, G. Gopakumar, R. K. Chaudhuri, B. P. Das, H. Merlitz, U. S. Mahapatra, and D. Mukherjee, Phys. Rev. A **68**, 040501(R) (2003).
[7] B. K. Sahoo, R. K. Chaudhuri, B. P. Das, H. Merlitz, and D. Mukherjee, Phys. Rev. A **72**, 032507 (2005).
[8] B. K. Sahoo, Phys. Rev. A **73**, 062501 (2006).
[9] B. K. Sahoo, Phys. Rev. A **80**, 012515 (2009).
[10] N. J. Stone, *Table of Nuclear Magnetic Dipole and Electric Quadruopole Moments*, IAEA Nuclear Data Section, Vienna International Centre, Vienna, Austria, April 2011 [http://www-nds.iaea.org/publications/indc/indc-nds-0594.pdf].
[11] G. W. Series, Phys. Rev. **105**, 1128 (1957).
[12] D. Sundholm and J. Oslen, J. Chem. Phys. **98**, 7152 (1993).
[13] Vladimir Kellö and Andrzej J. Sadlej, Chem. Phys. Lett. **292**, 403 (1998).
[14] P. Pyykkö, Mol. Phys. **106**, 1965 (2008).
[15] http://www.webelements.com/potassium/nmr.html.
[16] K. Blaum, W. Geithner, J. Lassen, P. Lievens, K. Marinova, and R. Neugart, CERN-PH-EP/2007-038 (2007).
[17] G. Neyens, Rep. Prog. Phys. **66**, 633 (2003).
[18] B. T. Feld, *Nuclear Electric Quadrupole Moments and Quadrupole Couplings in Molecules*, Nuclear Science Series, National Research Council (The National Academies Press, Washington, DC, 1949).
[19] L. A. Errico and M. Renteria, Phys. Rev. B **73**, 115125 (2006).
[20] K. Asahi and K. Matsuta, Nucl. Phys. A **693**, 63 (2001).
[21] G. Martinez-Pinedo, P. Schwerdtfeger, E. Caurier, K. Langanke, W. Nazarewicz, and T. Sohnel, Phys. Rev. Lett. **87**, 062701 (2001).
[22] C. Schwartz, Phys. Rev. **97**, 380 (1955).
[23] K. T. Cheng and W. J. Childs, Phys. Rev. A **31**, 2775 (1985).
[24] A. R. Edmonds, *Angular Momentum in Quantum Mechanics* (Princeton University Press, Princeton, 1996).
[25] P. J. C. Aerts and W. C. Nieuwpoort, Chem. Phys. Lett. **113**, 165 (1985).
[26] O. Visser, P. J. C. Aerts, D. Hegarty, and W. C. Nieuwpoort, Chem. Phys. Lett. **134**, 34 (1987).
[27] A. Mohanty and E. Clementi, in *Kinetically Balanced Geometric Gaussian Basis Set Calculations For Relativistic Many Electron Atoms*, Modern Techniques in Computational Chemistry: MOTECC-89, edited by E. Clementi (ESCOM, Leiden, 1989), Chap. 4, p. 169.
[28] R. E. Stanton and S. Havriliak, J. Chem. Phys. **81**, 1910 (1984).
[29] P. Ragavan, At. Data Nucl. Data Tables **42**, 189 (1969).
[30] I. Lindgren, Int. J. Quantum Chem. Symp. **12**, 33 (1978).
[31] D. Mukherjee and S. Pal, Adv. Quantum Chem. **20**, 281 (1989).
[32] U. Kaldor, J. Chem. Phys. **87**, 467 (1987); **87**, 4693 (1987).

[33] B. K. Sahoo, C. Sur, T. Beier, B. P. Das, R. K. Chaudhuri, and D. Mukherjee, Phys. Rev. A **75**, 042504 (2007).
[34] B. K. Sahoo, G. Gopakumar, R. K. Chaudhuri, B. P. Das, H. Merlitz, U. S. Mahapatra, and D. Mukherjee, Phys. Rev. A **68**, 040501(R) (2003).
[35] B. K. Sahoo, R. K. Chaudhuri, B. P. Das, S. Majumder, H. Merlitz, U. S. Mahapatra, and D. Mukherjee, J. Phys. B **36**, 1899 (2003).
[36] N. Bendali, H. T. Duong, and J. L. Vialle, J. Phys. B **14**, 4231 (1981).
[37] F. Touchard, P. Guimbal, S. Buttgenbach, R. Klapisch, M. D. S. Simon, J. M. Serre, C. Thibault, H. T. Duong, P. Juncar, S. Limberman, J. Pinard, and J. L. Vialle, Phys. Lett. B **108**, 169 (1982).
[38] A. Banerjee, D. Das, and V. Natarajan, Opt. Lett. **28**, 1579 (2003).
[39] J. Ney, R. Repnow, H. Bucke, and G. Schatz, Z. Phys. **213**, 192 (1968).
[40] R. W. Schmieder, A. Lurio, and W. Happer, Phys. Rev. **173**, 76 (1968).
[41] J. Ney, Z. Phys. **223**, 126 (1969).
[42] A. Sieradzan, A. Lurio, and W. Harper, Phys. Rev. **173**, 76 (1968).
[43] M. Glódź and M. Kraińska-Miszczak, J. Phys. B **18**, 1515 (1985).
[44] U. I. Safronova and M. S. Safronova, Phys. Rev. A **78**, 052504 (2008).
[45] P. Risberg, Ark. Fys. **10**, 583 (1956).
[46] R. M. Sternheimer and R. F. Peierls, Phys. Rev. A **3**, 837 (1971).
[47] S. Savanberg, Phys. Scr. **4**, 275 (1971).
[48] P. A. Bonczyk and V. W. Hughes, Phys. Rev. **161**, 15 (1967).
[49] E. P. Jones and S. R. Hartmann, Phys. Rev. B **6**, 757 (1972).
[50] A. Szabo and N. S. Ostlund, *Modern Quantum Chemistry* (Dover, New York, 1982).